Synchrophasor-Based Online Coherency Identification in Voltage Stability Assessment

Adeyemi Charles ADEWOLE, Raynitchka TZONEVA
Centre for Substation Automation and Energy Management Systems (CSAEMS)
Cape Peninsula University of Technology, P.O. Box 1906, Cape Town, South Africa
adewolea@cput.ac.za

***Abstract*—This paper presents and investigates a new measurement-based approach in the identification of coherent groups in load buses and synchronous generators for voltage stability assessment application in large interconnected power systems. A hybrid Calinski-Harabasz criterion and *k*-means clustering algorithm is developed for the determination of the cluster groups in the system. The proposed method is successfully validated by using the New England 39-bus test system. Also, the performance of the voltage stability assessment algorithm using wide area synchrophasor measurements from the key synchronous generator in each respective cluster was tested online for the prediction of the system's margin to voltage collapse using a testbed comprising of a Programmable Logic Controller (PLC) in a hardware-in-the-loop configuration with the Real-Time Digital Simulator (RTDS) and Phasor Measurement Units (PMUs).**

***Index Terms*—Clustering method, machine learning, phasor measurement unit, power system stability, voltage stability.**

I. INTRODUCTION

The continuous operation of power systems beyond their design limits due to load increase without a concomitant increase in generation and transmission capacities results to the operation of the power system in a stressed state. Thus, power system instabilities such as voltage instability/voltage collapse are inevitable.

Voltage instability refers to the inability of the power system to maintain acceptable voltage levels at all buses in the system. This can be caused by the loss of voltage control and restriction to reactive power transfer to the critical buses in the reactive power deficit area [1-2].

In order to prevent voltage instability/voltage collapse, it is necessary to have in place stability indices which can be used to monitor and provide situational awareness of the power system. This can be done by using bus/line loadability indices [3-5], or indices relating to reactive power reserve at the load or generator buses [2], [6-11].

Indices derived from the Reactive Power Reserves (RPRs) at the generators were shown to be effective for voltage stability assessment [2], [6-11], since the reactive power from synchronous generators is the primary source of voltage control in the power system. Thus, the availability of adequate level of the RPR is an indication that the system is stable and operating within acceptable system limits.

Therefore, in order to adequately monitor voltage stability in a power system, it is necessary to determine the particular synchronous generator(s) providing voltage control at the load buses for various system operating conditions.

This research was funded by the South African National Research Foundation (NRF) THRIP Grant 201106110000.

A set of generators providing voltage control for a set of critical load buses or area belongs to a coherent group, and functions as a Reactive Power Reserve Basin (RPRB) for those load buses [2]. This provides a less complex, but practical way of determining the state of the power system and its margin to voltage instability.

The traditional application of coherency grouping in power system has been in the development of reduced order models for the decomposition of large power system models into smaller, less complex equivalent systems [12-15]. The use of reduced equivalent models allows power system analysis to be less complex, with less computational effort especially when a large number of scenarios need to be studied. Generator coherency analysis was used in [16-21] for transient stability studies. Other applications of coherency grouping include oscillation detection [22], vulnerability assessment [23], fault event location [24], etc. However, coherency grouping methods for reduced order models, transient stability studies, oscillation detection, vulnerability assessment, etc would fail when applied in voltage stability assessment because the sequence of events leading to power system oscillation or transient instability are different for voltage instability. Also, the system variables used in transient stability studies, oscillation detection, vulnerability assessment, etc are mainly generator speed, generator rotor angles, or other generator swing-related variables. Exploratory simulations carried out by the authors have shown that these variables are poor indicators of voltage instability. Furthermore, for the voltage stability assessment of a purely voltage stability condition, it is only at the unstable state (voltage collapse point) that generators tend to accelerate and swing against each other. However, control actions are usually unpredictable when implemented in the unstable region of the power system. Thus, the system must be monitored continuously and control actions should be initiated at the system 'alert' state before the system becomes unstable.

Voltage stability assessment algorithms are used in the monitoring of power systems and detecting voltage stability threats. When the system tends towards voltage instability, timely remedial actions are taken to avoid instability. The Real-time Voltage Stability Assessment (RVSA) index proposed by the authors in [10] is based on the monitoring of variables derived from key generators in the power system. Coherency clustering of generators in a large interconnected power system can be used to provide an indication of the system's margin to voltage instability. In this regard, the key generator in each cluster can be taken as representative of the primary RPR source for each Voltage

Digital Object Identifier 10.4316/AECE.2015.04005

Control Area (VCA) in the power system.

A literature survey carried out showed that very few literature exists on coherency grouping for voltage stability assessment. This is probably due to the complex nature of analyzing voltage instability and the mechanisms causing it such as system loading, the operation of Under-Load Tap-Changer (ULTC) of transformers, the operation of Over-Excitation Limiters (OXL), presence of dynamic loads, etc.

An algorithm for clustering the generators in the system into RPR basins by using the Jacobian of the reactive power and voltage was described in [2]. The partitioning method by [25] is based on voltage variation at each load bus with respect to real power and reactive power variations at the other load buses. The real and reactive powers at the load buses of interest are related to the voltage level by computing the reduced Jacobian of the load flow.

The generator coherency method proposed by [18] for transient stability study was modified by [26] and applied to generator coherency for voltage stability studies. The clustering method by [26] is also based on the reduced Jacobian matrix and modal analysis of the system load flow. A method based on sensitivities derived from the reactive power flowing in a line in relation to the reactive power injection at a load bus was suggested in [27]. The method considered in [28] made use of eigenvalues from modal-analysis and the shuffled frog-leaping algorithm.

The limitation of these existing methods is that computation of the reduced Jacobian is required for each load bus in the system. Also, the use of eigenvalues in the modal analysis requires multiple load flow studies for each operating point. This is rather time consuming for a large system. An assumption made by [28] is that the clustering needed to be done only once. However, a sequence of events can lead to cascading effects resulting to voltage instability of the power system. This combination of cascading disturbances would likely result to the formation of a group of clusters different from the original one. In addition, online wide area protection and control schemes would require fast real-time coherency analysis to be carried out. This is easily satisfied by using a measurement-based method. With the introduction of wide-area measurements from Phasor Measurement Units (PMUs), measurement-based techniques have been suggested for application in coherency grouping in transient stability studies [20-21], dynamic vulnerability assessment [23], event location after a disturbance [24], etc. However, PMU-related hardware was not used by [20-21], [23-24]. Rather, assumptions were wrongly made that the time-domain simulation measurements from MATLAB/Simulink, SIMPOW®, DSA-PowerTools (from Powertech Labs), etc are equivalent to the synchrophasor measurements from PMUs. In reality, what distinguishes synchrophasor measurements from other measurement types include the measurement algorithm used in the estimation of the synchrophasors, type of filter, reporting rates, data transfer using Ethernet communication network, compliance to the measurement and performance requirements as specified in the IEEE C37.118 standard [29-31], etc.

From the foregoing, it can be seen that it is necessary to implement a clustering algorithm for application in voltage stability studies in real-time. Also, actual measurements from PMUs should be used in such research.

The contributions of this paper include the following:

(i) the online identification of the coherent load buses and generator groups for voltage stability assessment in large power systems, performed with reduced computational burden; (ii) the novel application of measurement-based clustering approach for voltage stability studies; (iii) the development of a hybrid Calinski-Harabasz criterion and *k*-means algorithm to determine the optimal number of clusters before the application of the clustering algorithm; (iv) extension of the authors' work [10] on the key generator principle to multi-area interconnected power systems, (v) the use of actual synchrophasor measurements synchronized to a GPS time source and streamed onto a communication network for load and generator clustering, and voltage stability assessment; and (vi) the implementation and testing of the proposed method using a lab-scale testbed.

The rest of this paper is organized as follows: Section II presents an overview of the proposed method. The implementation of the proposed method is given in Section III. Section IV presents and discusses the results obtained. The conclusion of the paper is summarized in Section V.

II. Overview of the Proposed Coherency-Based Method

The proposed coherency-based method involves the following algorithms: (a) A measurement-based hybrid Calinski-Harabasz criterion and *k*-means algorithm for clustering the load buses and the generators in the system into VCAs and RPRBs respectively; and (b) the extension of the authors' work on real-time voltage stability assessment [10] to a multi-area power system

A. Hybrid Clustering Algorithms

Clustering is an unsupervised learning algorithm which is used to discover pattern within a set of objects. Thus, similar objects are grouped to the same cluster based on the similarities observed, with objects belonging to the same cluster sharing similar properties with one another. Conversely, objects belonging to different clusters share less similarities together.

Clustering algorithms can be broadly classified into two types: (1) hierarchical algorithms; and (2) partitioning algorithms [32-34].

Partitioning algorithms group objects into a given number of cluster groups, and exchange the objects between the groups until a certain criterion is optimized. Examples of partitioning algorithms are the *k*-means algorithm and the Gaussian Mixture (GM) model.

k-means algorithm partitions the objects into pre-selected *k* mutually exclusive clusters by searching for partitions in which objects within each partition are closer to each other, and far from objects in other partitions.

The centroid for the respective clusters is the point that has the minimum summation distance from all objects in that cluster. An iterative algorithm is used to minimize the sum of the distances to the cluster centroid by exchanging objects between the clusters until the minimum sum is obtained. The Euclidean distance is the length of the line segment between two points *A* and *B*.

This is given as [34]:

$$\|A-B\| = \sqrt{(A_1-B_1)^2+(A_2-B_2)^2+...+(A_n-B_n)^2} \quad (1)$$

The GM model is a parametric function based on probability and an assumption that all data points are from a mixture of a finite number of Gaussian distributions with unknown parameters. It uses an iterative algorithm in selecting the component that maximizes the posterior probability.

The *k*-means algorithm was chosen for the implementation of the coherency algorithm used in this paper because it is non-hierarchical, non-overlapping, has faster convergence, memory-efficient, good for large amount of data, and easy to understand the results [34].

The steps involved in the realization of the *k*-means algorithm as implemented in MATLAB [34] are given below:

Step 1: Choose the number of clusters *k* to partition the objects in the data into.

Step 2: Read the input data.

Step 3: Obtain the cluster centroids.

Step 4: Calculate the distance between the objects in the data and the cluster centroids.

Step 5: Allocate the objects to the nearest cluster.

Step 6: Repeat Steps 3-5 until the stopping criteria is satisfied.

The stopping criteria can be: (1) the number of iterations; (2) no change in the vectors of the centroid over an iteration threshold; and (3) no changes in the cluster membership.

The shortcoming of the *k*-means algorithm is that the number of clusters *k* needs to be known beforehand. One solution to this is the use of the Calinski-Harabasz Criterion (CHC) (Variance Ratio Criterion) in the determination of the optimal number of clusters.

The Calinski-Harabasz criterion is given as [35]:

$$CHC_k = \frac{SS_B}{SS_W} \times \frac{(N-k)}{(k-1)},\ k = \overline{1,K} \quad (2)$$

where SS_B is the overall variance between the clusters, SS_W is the overall variance within the cluster, k is the number of clusters, and N is the number of observations.

$$SS_B = \sum_{i=1}^{K} n_i \left\| m_i - m \right\|^2 \quad (3)$$

$$SS_w = \sum_{i=1}^{K} \sum_{x \in c_i} \left\| x - m_i \right\|^2 \quad (4)$$

where m_i is the centroid of the ith cluster, m is the mean of the data, n_i is the number of points in the ith cluster, x is the data point, C_i is the ith cluster, $\left\| m_i - m \right\|$ and $\left\| x - m_i \right\|$ are the Euclidean distances between the two vectors respectively, K is the number of synchronous generators in the system, and it is used as the maximum number of clusters to consider.

The optimal number of clusters is obtained by maximizing CHC_k with respect to the number of clusters k. This is because the best partitioning is obtained with the largest CHC_k possible by using a large SS_B and a small SS_W.

The Calinski-Harabasz criterion and the *k*-means algorithm are combined in this paper. The flowchart for the proposed hybrid *k*-means clustering algorithm is summarized in Fig. 1.

where V is a vector of the CHC_k values for $i = \overline{1,K}$.

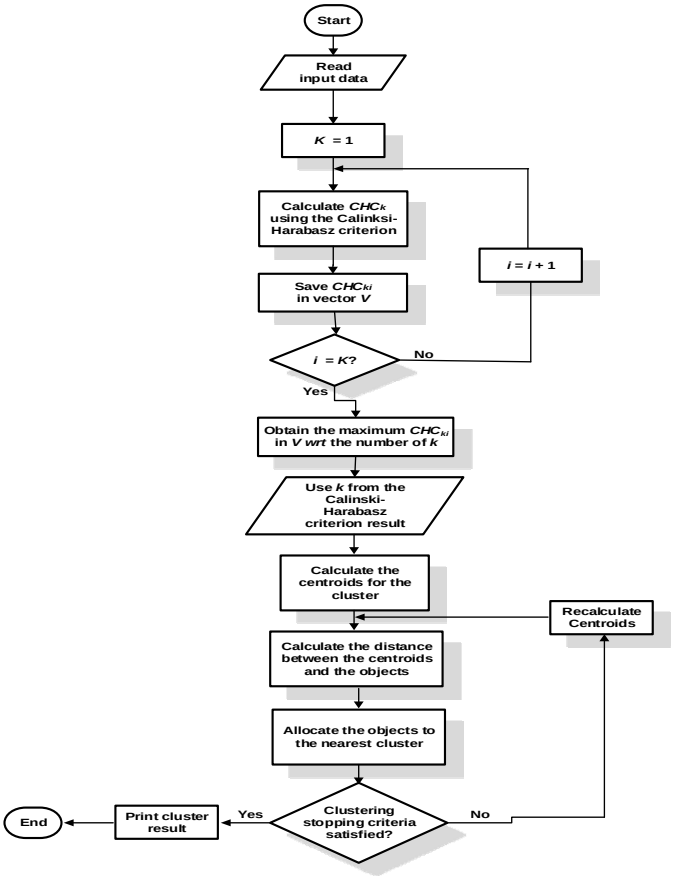

Figure 1. Proposed algorithm using a hybrid Calinski-Harabasz criterion and *k*-means clustering

In addition to the CHC, another performance index used in the evaluation of the obtained cluster was the silhouette coefficient *s*. The silhouette coefficient relates to how well-defined the cluster is and the proximity of points in one cluster to points in the neighbouring clusters. The coefficient is made up of the mean distance (*a*) between an object and all other points in the same cluster, and the mean distance (*b*) between an object and all other points in the next neighbouring cluster(s).

The silhouette coefficient (*s*) is given as [34]:

$$s = \frac{b-a}{\max(a,b)}, \quad -1 \le s \le 1 \quad (5)$$

A well partitioned cluster groups should have positive silhouette coefficients, with objects within a cluster group having values in close proximity to each other.

B. Real-Time Voltage Stability Assessment (RVSA) Index

The concept of Voltage Control Areas (VCAs) and Reactive Power Reserve Basins (RPRBs) was presented by [2]. It is based on the premise that the load buses in a power system can be partitioned into groups of buses with similar voltage profile or/and unique voltage collapse problem. These coherent load buses are referred to as belonging to the same VCA. A set of generators providing reactive power support to a particular VCA are referred to as the RPRB for that VCA. This implies that generators within a particular RPRB would have their RPR exhausted as it attempts to provide voltage control during contingencies or changes in the system operating condition.

The reactive power margin in a VCA has been used in [2], [36-39] to provide an indication of the state of power systems. In particular, [37], [39-40] used the key generator concept whereby the voltage stability index is based on the variables measured at the key generators in the power system.

The maximum reactive power Q_{max} at a synchronous generator is given as [1], [11]:

$$Q_{\max} = -\frac{V_g^2}{X_s} + \sqrt{\frac{V_g^2 I_{fd\max}^2}{X_s^2} - P_{g\max}^2} \quad (6)$$

where V_g is the generator terminal voltage, I_{fdmax} is the maximum field current, X_s is the synchronous reactance, and P_{gmax} is the maximum real power of the generator.

The Effective Generator Reactive Power Reserve (EGRPR) is said to be the difference between the reactive power output of the synchronous generator at the point of voltage collapse and its reactive power output at the *j*th operating time [9], [39]. This is in contrast to the Technical Generator Reactive Power Reserve (TGRPR) in which the maximum reactive power obtainable is based on the capability curve of the generator. A comparative analysis on EGRPR and TGRPR is given in [41].

Mathematically, the EGRPR is given as:

$$EGRPR = Q_{\max}^c - Q_{gj} \quad (7)$$

where $Q_{\max}^c$ is the maximum generator reactive power at the point of voltage collapse, Q_{gj} is the reactive power in MVAr of the synchronous generator at the current operating point *j*.

From the definition of the EGRPR, it can be inferred that at the point of voltage collapse,

EGRPR = 0, as $Q_{g\max}^c = Q_{gj}$, $P_{g\max}^c = P_{gj}$.

Therefore,

$$-\frac{V_g^2}{X_s} + \sqrt{\frac{V_g^2 I_{fd\max}^{c2}}{X_s^2} - P_{g\max}^2} = -\frac{V_g^2}{X_s} + \sqrt{\frac{V_g^2 I_{fdj}^2}{X_s^2} - P_{gj}^2} \quad (8)$$

where $I_{fd\max}^c$ is the maximum field current of the synchronous generator at the point of collapse, I_{fdj} is the field current of the synchronous generator at the *j*th operating time.

From (8),

$$\frac{I_{fdj}}{I_{fd\max}^c} = 1 \quad (9)$$

Thus, the Effective Generator Field Current Reserve (EGFCR) based on generator field current is equivalent to the EGRPR, and is given as:

$$I_{fdm} = I_{fd\max}^c - I_{fdj} \quad (10)$$

The Real-Time Voltage Stability Assessment (RVSA) index for the prediction of the system's margin to voltage instability/collapse is formulated as:

$$RVSA_{Ifd} = \left(\frac{I_{fdm}}{I_{fd\max}^c}\right) \times 100\ \% \quad (11)$$

$$RVSA_{Ifd} = \left(1 - \frac{I_{fdj}}{I_{fd\max}^c}\right) \times 100\ \% \quad (12)$$

The $RVSA_{Ifd}$ index obtained in (12) is applied to the clusters obtained from the *k*-means algorithm. In this, the $RVSA_{Ifd}$ index of the key generator in each cluster can be monitored to provide situational awareness of the power system.

For a large interconnected power system, a wide area $RVSA_{Ifd,\ sys}$ index for a multi-area power system partitioned into *k* clusters is proposed to be:

$$RVSA_{Ifd,sys} = \min_{l \in sys}\left\{\mathrm{RVSA}_{Ifd,l},\ l = \overline{1,k}\right\} \quad (13)$$

$$= \min_{l \in sys}\left\{\left(1 - \frac{I_{fdj}^l}{I_{Ifd\max,l}^{c,l}}\right) \times 100\,\%,\ l = \overline{1,k^*}\right\} \quad (14)$$

where k^* is the optimal number of clusters.

This implies that the state of the power system is obtained by using the minimum $RVSA_{Ifd}$ index of the key generator in any of the clusters.

The proposed hybrid algorithm and the multi-area $RVSA_{Ifd,sys}$ index for real-time voltage stability assessment of a multi-area system based on PMU measurements is shown in Fig. 2.

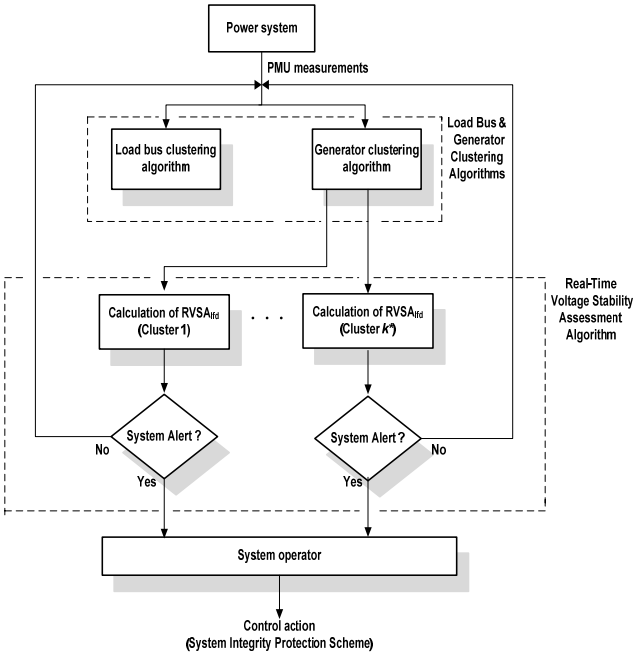

Figure 2. Real-time implementation of the proposed method

III. Implementation of the Proposed Method

The proposed method presented in Section II is implemented using the developed Wide Area Monitoring, Protection and Control (WAMPAC) testbed located at the Centre for Substation Automation and Energy Management Systems (CSAEMS), at the Cape Peninsula University of Technology (CPUT). The equipment used include the Real-Time Digital Simulator® (RTDS), Phasor Measurement Units (PMUs), Phasor Data Concentrators (PDCs), GPS satellite clock, SEL-3378 Synchrophasor Vector Processor (SVP), and industrial network switches. The lab-scale testbed is illustrated in Fig. 3.

The RTDS is used for the real-time simulation of the power system network with a 50 microsecond time-step. The GPS satellite clock is used in the provision of time synchronization to the various components of the testbed.

The synchrophasor measurements from the external PMU hardware and the RTDS-GTNET-PMU module are published onto an Ethernet communication infrastructure. The substation PDC (SEL-3378 SVP) collects and time-aligns the synchrophasor measurements based on their time-stamps. The SEL-3378 SVP was also configured as a Programmable Logic Controller (PLC) to execute the RVSA algorithm. The synchrophasor output from the SEL-3378 is published onto a higher level network.

The regional PDC (SEL-5073) collects, time-aligns, and archives the synchrophasor measurements at the regional level for real-time and offline applications respectively.

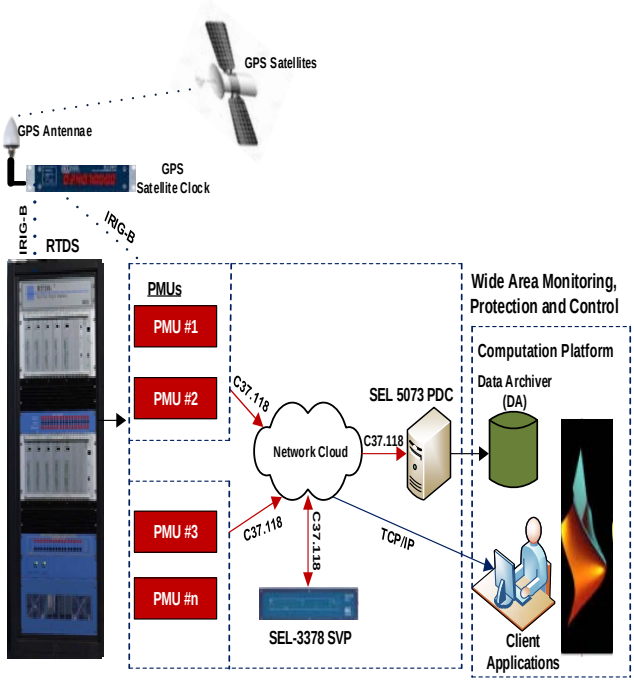

Figure 3. WAMPAC lab-scale implementation testbed

A. *Study Network*

The study network used is the New England 39-bus test system [42]. This network consists of 10 generators, 39 buses, 34 transmission lines, and 19 loads. The RTDS-RSCAD software is used in the modelling of the study network. The generators are connected to buses 30-39, and are equipped with IEEE Type-1 excitation systems and governors. The transformer between buses 11 and 12 is modified to include an Under-Load Tap Changer (ULTC). Also, generator G3 is modified to include an OverExcitation Limiter (OXL). The parameters for the transformer ULTC and OXL are given in the appendix. PMUs are sited at each of the generator buses and at the critical load buses in the network. Table I gives the configuration used for each PMU.

TABLE I. PMU CONFIGURATION

Configuration	Parameter
Performance class	Class P
Configuration frame format	Config-2
Station name	16 characters
PMU hardware ID	1-65534
PMU output port number	1-65535
Reporting rate	60 fps
Phasor format	Real
Phasor output format	Polar
Phasor output	Positive sequence bus voltages and currents
Analogue format	Real

B. *Simulations*

The coherency identification approach in this paper is based on the principle that for any voltage stability related event, certain group of generators tends to respond by providing reactive power support/voltage control of the load buses or stressed area.

Therefore, two or more generators are voltage stability coherent if their terminal measurements dynamically respond to voltage stability related events and have their reactive power margin exhausted during such events. Similarly, coherent load buses are the buses with similar voltage profile. An event on any of the load buses belonging to a coherent group results to changes in the other load buses within the group.

Four case studies relating to the use of synchrophasor measurements in load and generator coherency clustering are investigated.

These cases are: (1) load bus clustering; (2) generator clustering; (3) generator clustering with OXL action; and (4) the effects of PMU reporting rates on generator clustering.

In order to drive the system towards its 'alert' state and determine the corresponding generators in the RPRBs, an increased loading condition involving increments in the real power (ΔP) and reactive power (ΔQ) at a constant power factor is carried out at all the load buses in the VCA of interest. This is done with the real and reactive powers of the loads in the other clusters constant.

It should be noted that for the case studies considered in this paper, 10% load increase at the load buses of interest is carried out every 60 s. 180 s measurement window corresponding to the third consecutive load increase is used in order to account for voltage deviations up to the third level of load increase. This is equivalent to the measurements for a stressed system in the 'alert' state. The number of measurements equals (*60fps x 180s)* synchrophasor measurement points. Table II gives the PMUs used, and the various measurements published by them.

TABLE II. MEASUREMENT ACQUISITION BY PMUS

PMU locations	Phasor measurements	Analogue measurement	PMU digital
Load buses	Positive sequence of voltage and current	Real power, reactive power	Line breaker status
Generator buses	Positive sequence of voltage and current	Real power, reactive power, generator field current, generator rotor speed	Gen. status

IV. RESULTS AND DISCUSSION

A. *Case Study 1: Load Bus Clustering*

Fig. 4 shows the RSCAD-Runtime bus voltages for the steady-state and system loading conditions respectively. At steady-state condition, load buses 4, 7, 8, 12, and 20 already have Voltage Per Unit (Vp.u.) below 1.0 Vp.u. However, the Vp.u. at these buses was still within the acceptable limit for the steady-state condition. Stressing the system by increasing the loading at the buses mentioned above, is capable of causing the voltage at the load buses to drop below the acceptable level with the system going into its 'alert' state and consequently resulting to voltage collapse.

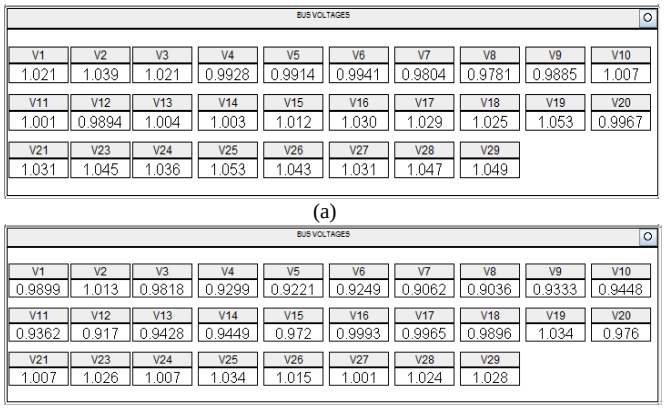

Figure 4. RSCAD-Runtime measurement palette for (a) Vp.u. at the steady-state condition; and (b) under system loading conditions

The hybrid Calinski-Harabasz criterion and *k*-means clustering algorithm was applied to the synchrophasor measurements of the bus voltages obtained from an increased system loading condition similar to that in Fig. 4b. Fig. 5 shows the plot of the Calinski-Harabasz criterion for various clusters *k*. The optimal number of *k* is 4. Table III gives the buses in each cluster. Cluster 1 (in bold) in Table III is identified for further studies relating to the generator coherency identification.

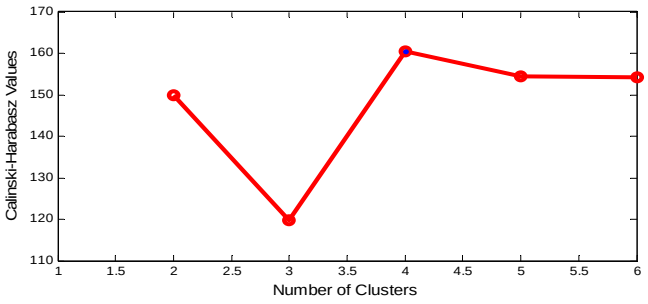

Figure 5. Plot of Calinski-Harabasz index for the synchrophasor measurements at the load buses

TABLE III. CLUSTER GROUPS FOR THE LOAD BUSES

Cluster number	Cluster	Load buses
Cluster 1	**{4, 5, 6, 7, 8, 9, 10, 11, 12, 13, 14}**	**{4, 7, 8, 12}**
Cluster 2	{1, 3, 18}	{3, 18}
Cluster 3	{2, 15, 16, 17, 20, 21, 24, 26, 27}	{15, 16, 20, 21, 24, 26, 27}
Cluster 4	{19, 23, 25, 28, 29}	{23, 25, 28, 29}

Cluster 1 was chosen for further analysis because it is the most critical VCA in the study network and is capable of driving the system into voltage instability. The single line diagram of the study network showing the study area in this paper is given in Fig. 6.

B. Case Study 2: Generator Clustering

Case study 2 was carried out in order to investigate the best variables for generator coherency, and to identify the RPRB providing voltage control/reactive power support at the VCA identified in case study 1.

A study was carried out using simultaneous load increase at the load buses in cluster 1 of Table III {4, 7, 8, and 12}. Increased loading at these buses results to a voltage collapse at the 4th load increase. Figs. 7-8 show the terminal voltages and the field currents (I_{fd}) for generators G1-G4.

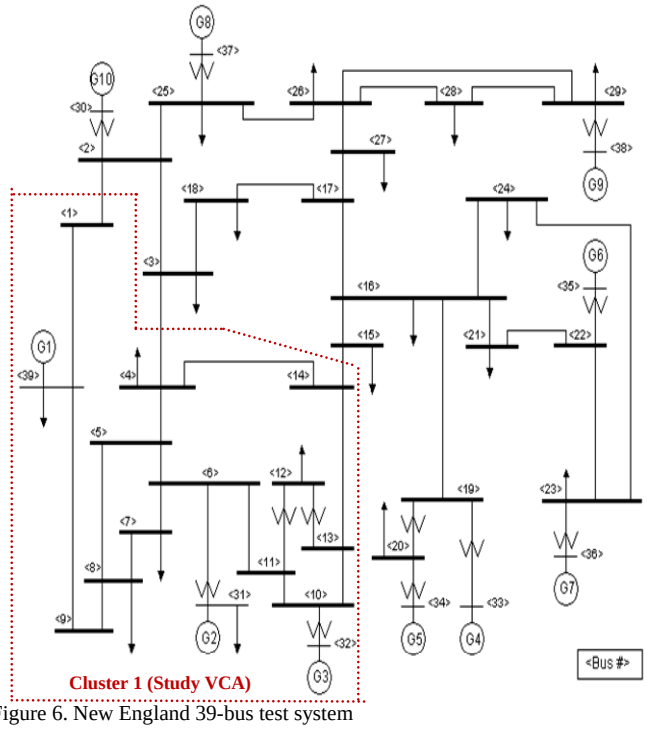

Figure 6. New England 39-bus test system

Although, generator G4 does not belong to the RPRB in cluster 1, it was the most responsive of the external generators not in cluster 1. Therefore, the plot of generator G4 terminal voltage was added in this figure to show that the response of the generators in other clusters can be ignored since these external generators do no exhaust their RPR.

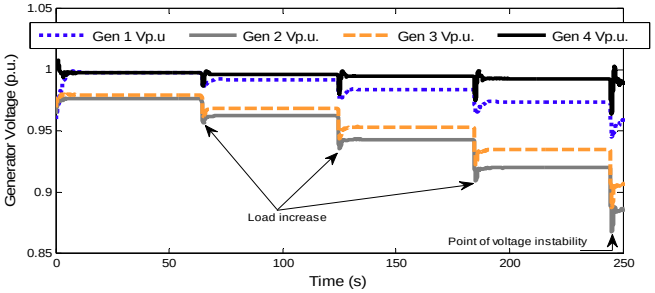

Figure 7. Terminal voltages for generators G1-G4

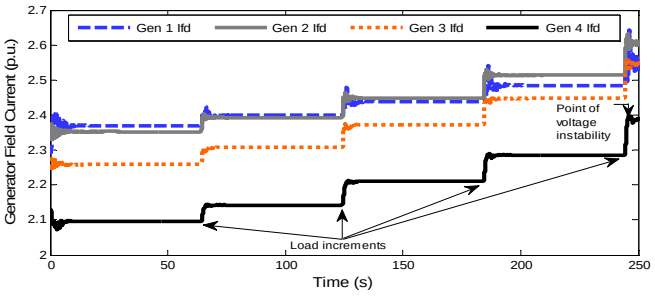

Figure 8. Field currents for generators G1-G4

From Figs. 7-8, it can be seen that the most stressed generators are generators G2 and G3 as shown by the drop in generator terminal voltages and the increase in the generator field currents respectively.

Seven generator/generator-derived variables were investigated to determine the best variable for the generator clustering algorithm with respect to the voltage stability assessment algorithm.

These are: (1) Generator reactive power (MVAr); (2) generator field current (I_{fd}); (3) generator stator current (I_{st}); (4) generator terminal voltage (V_g); (5) generator rotor speed (Rad./sec.); (6) Real-Time Voltage Stability Assessment Index using generator field current reserve $RVSA_{Ifd}$; and (7) Real-Time Voltage Stability Assessment Index using generator reactive power reserve $RVSA_Q$ proposed in [36-39].

Fig. 9 shows the plots of the Calinski-Harabasz index for the above-mentioned variables. From Fig. 9, it can be seen that the highest Calinski-Harabasz value was obtained using the $RVSA_{Ifd}$ index obtained from the generator field current.

The final decision on the best variable to use was based on the number of clusters and the silhouette coefficients obtained. Fig. 10 shows the silhouette plot for $RVSA_{Ifd}$ variable.

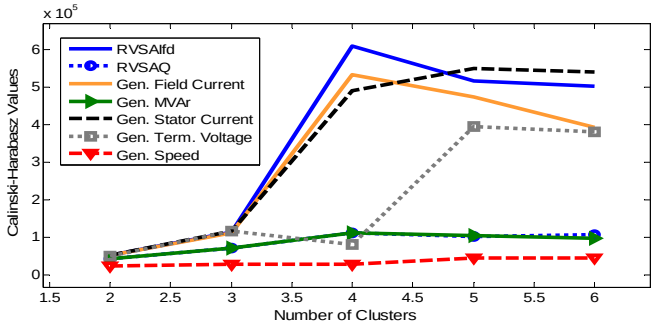

Figure 9. Plot of Calinski-Harabasz index for various generator variables

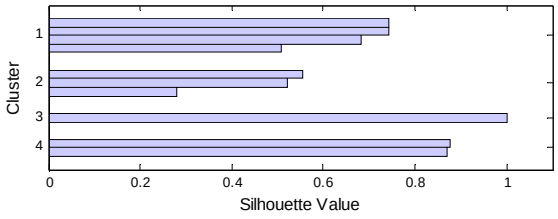

Figure 10. Silhouette plot obtained using $RVSA_{Ifd}$ variable

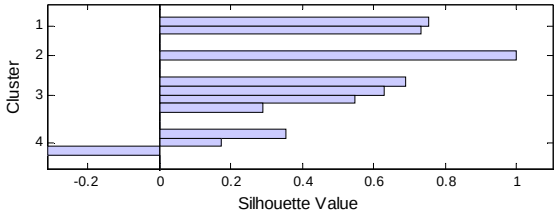

Figure 11. Silhouette plot obtained using MVAr variables

Compared with Fig. 11 obtained using generator reactive power variables, it can be seen that all the generators in the clusters have positive silhouette values in Fig. 10, while Fig. 11 has a generator with a negative silhouette coefficient in cluster 4.

Table IV shows the generators in each cluster for an increased loading scenario at the load buses given in cluster 1 of Table III. From Table IV, it can be seen that the generators in the study network have been clustered into 4/5 coherency groups depending on the variable used.

In bold text is the acceptable cluster group for the case being investigated based on the values of the CHC, the number of clusters, and the silhouette coefficients obtained.

TABLE IV. CLUSTER GROUPS FOR THE SYSTEM GENERATORS FOR VARIOUS VARIABLE TYPES

Variable type	Number of clusters	Generator cluster
Generator reactive power (MVAr)	4	{1, 3}; {4, 5, 7}; {8, 9}; {2, 6, 10}
Generator field current (I_{fd})	4	{1, 2, 3}; {4, 6, 7, 8, 9}; {5}; {10}
Generator stator current (I_{st})	5	{2, 3, 4}; {5, 8}; {1}; {10}; {7}
Generator terminal voltage (V_g)	5	{2, 3}; {4, 5}; {8, 10}; {1}; {7}
Generator rotor speed (Rad./sec)	5	{4, 5, 6, 7, 9}; {8, 10}; {1}; {2}; {3}
$RVSA_{Ifd}$	4	**{1, 2, 3}; {4, 7, 8, 10}; {6, 9}; {5}**
$RVSA_Q$	4	{1, 2, 3, 6}; {4, 5, 10}; {8, 9}; {7}

C. *Case Study 3: Generator Clustering With OXL Action*

In case study 3, the transformer between buses 11 and 12 was modified to include an ULTC. Also, an OXL was incorporated into generator G3. This was done in order to investigate the effect of ULTC and OXL actions on the clustering algorithm.

Fig. 12 shows the generator field currents for the system loading scenario (in case study 2) and the operation of the OXL at generator G3. It can be seen that there was an increase in generator G2 field current as a result of the ramping down of generator G3 field current due by the OXL.

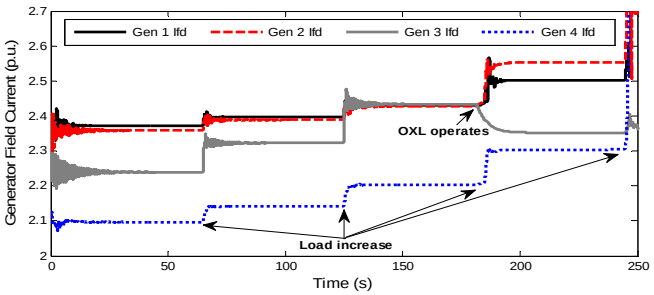

Figure 12. Field currents for generators G1-G4 (case study 3)

The clustering result for this case study is ({1, 2}; {3, 6, 9}; {4, 7, 8, 10}; {5}). Compared to the result obtained in Table IV, it can be seen that G3 has been reassigned to the cluster group {6, 9}. Fig. 13 shows the plot of the silhouette coefficients for case study 3 with OXL action.

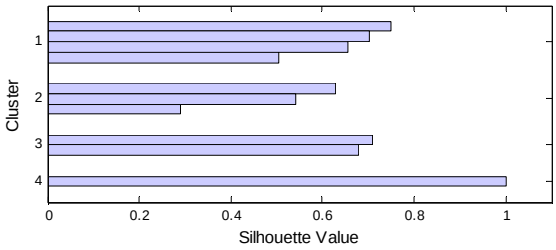

Figure 13. Silhouette plot obtained for case study 3 using $RVSA_{Ifd}$ variables

This further shows that coherency clustering in VCAs and RPRBs for VSA need to consider the effects of system dynamics like ULTC and OXL actions. Also, a once-off approach proposed in [28] would fail in this case.

D. Case Study 4: The Effects of PMU Reporting Rates

The effect of the various PMU reporting rates on generator clustering was investigated for the increased loading scenario at the load buses in cluster 1 of Table III.

The Calinski-Harabasz and silhouette values for each reporting rate were computed. Fig. 14 shows the plots for the Calinski-Harabasz values for various PMU reporting rates.

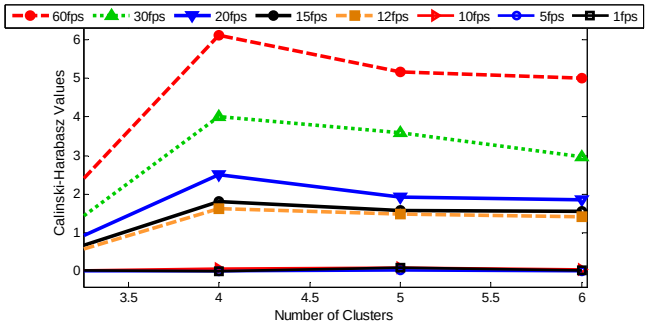

Figure 14. Plot of CHC for various PMU reporting rates

From Fig. 14, it can be seen that the highest Calinski-Harabasz values were obtained for the 60 fps reporting rate. Reporting rates higher than 60 fps could not be used because the substation PDC (SEL-3378 SVP) has a maximum reporting rate of 60 fps, even though higher reporting rates were possible with the PMUs and the regional PDC (SEL-5073). Table V shows the various generator clusters obtained for various PMU reporting rates using the $RVSA_{Ifd}$ index.

TABLE V. CLUSTER GROUPS FOR VARIOUS PMU REPORTING RATES

Reporting rate (fps)	Number of clusters	Generator cluster
60	4	**{1, 2, 3}; {4, 7, 8, 10}; {6, 9}; {5}**
30	4	{1, 2, 5}; {4, 7, 8, 10}; {6, 9}; {3}
20	4	{1, 2, 3, 5}; {4, 7, 8, 10}; {6}; {9}
15	4	{1, 2, 3, 5}; {4, 8, 10}; {6, 9}; {7}
12	4	{1, 2, 5}; {4, 7, 8, 10}; {6, 9}; {4}
10	5	{1, 2, 3}; {4, 8, 10}; {6, 9}; {5}; {7}
5	5	{1, 2, 5}; {4, 8, 10}; {6, 9}; {3}; {7}
1	5	{1, 2, 3}; {4, 7, 8}; {6, 9}; {5}; {10}

E. Application of the $RVSA_{Ifd,sys}$ Index to the Coherency Result using the Lab-Scale Testbed

The wide area voltage stability index proposed in (14) above can be applied to the key generator in each cluster to provide an indication of the system's margin to voltage collapse. The minimum $RVSA_{Ifd}$ index of the key generator in any of the clusters is taken as the system's margin to voltage collapse.

The index is applied in real-time using the lab-scale testbed given in Fig. 3. Fig. 15 shows the real-time plots of the $RVSA_{Ifd,sys}$ index for the key generators {G2, G4, G5, 6} in clusters 1-4 for increased loading conditions at the load buses 4, 7, 8, 12. From Fig. 15, the lowest RVSA index is observed to be that from generator 2, which is the key generator in cluster 1. From the figure, it can be seen that the system collapses at the fourth load increase as indicated by the $RVSA_{Ifd,sys}$ index of generator 2.

From the foregoing, it can be seen that the proposed coherency clustering approach facilitates the monitoring of interconnected large-scale power system using a reduced set of measurements from the key generator in each cluster. This reduces tremendously the number of PMUs required, input variables, computational resources and time required for power system monitoring and situational awareness.

V. CONCLUSION

This paper presented an online clustering approach for application in voltage stability assessment. In contrast to conventional model-based methods, the proposed approach is based on system variables directly obtained from synchrophasor measurements from PMUs.

Simulations were carried out on the New England 39-bus test system. Cluster validity measures were used to validate the coherency results obtained for the load and generator buses in the test system.

The simulation scenarios considered include increased loading conditions, the effects of transformer ULTC and generator OXL. It is shown that the determination of the generator clusters is not static, but rather a dynamic task that should be done in real-time as the system conditions changes.

Also, the effects of PMU reporting rates were investigated, and it was shown that the use of 60 fps gave the best results for the cases considered. Furthermore, the cluster results obtained were applied to a lab-scale testbed for online voltage stability assessment.

The simplicity, accuracy, and reduced computational burden of this measurement-based approach validates and shows that it can be applied in real-time System Integrity Protection Schemes (SIPS) for mitigating voltage collapse.

APPENDIX A

The OXL at generator G3 is calculated using the recommendations in [1], and it is as shown in Fig. A1. The parameters used are given in Table A1.

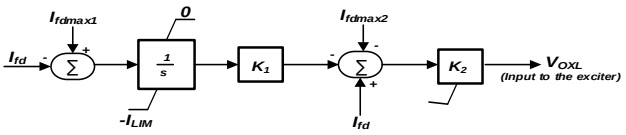

Figure A1. Block diagram of OXL used at generator 3 for case study 3

TABLE A1. GENERATOR 3 OXL PARAMETERS

I_{fdmax1} (p.u.)	I_{fdmax2} (p.u.)	I_{LIM} (p.u.)	K_1	K_2
2.352	3.584	11.0	0.248	12.6

where I_{fd} is the generator field current at the current operating time, I_{fdmax1} and I_{fdmax2} are the maximum field current limits for stages 1 and 2 of the generator OXL respectively. Further details are available in [1].

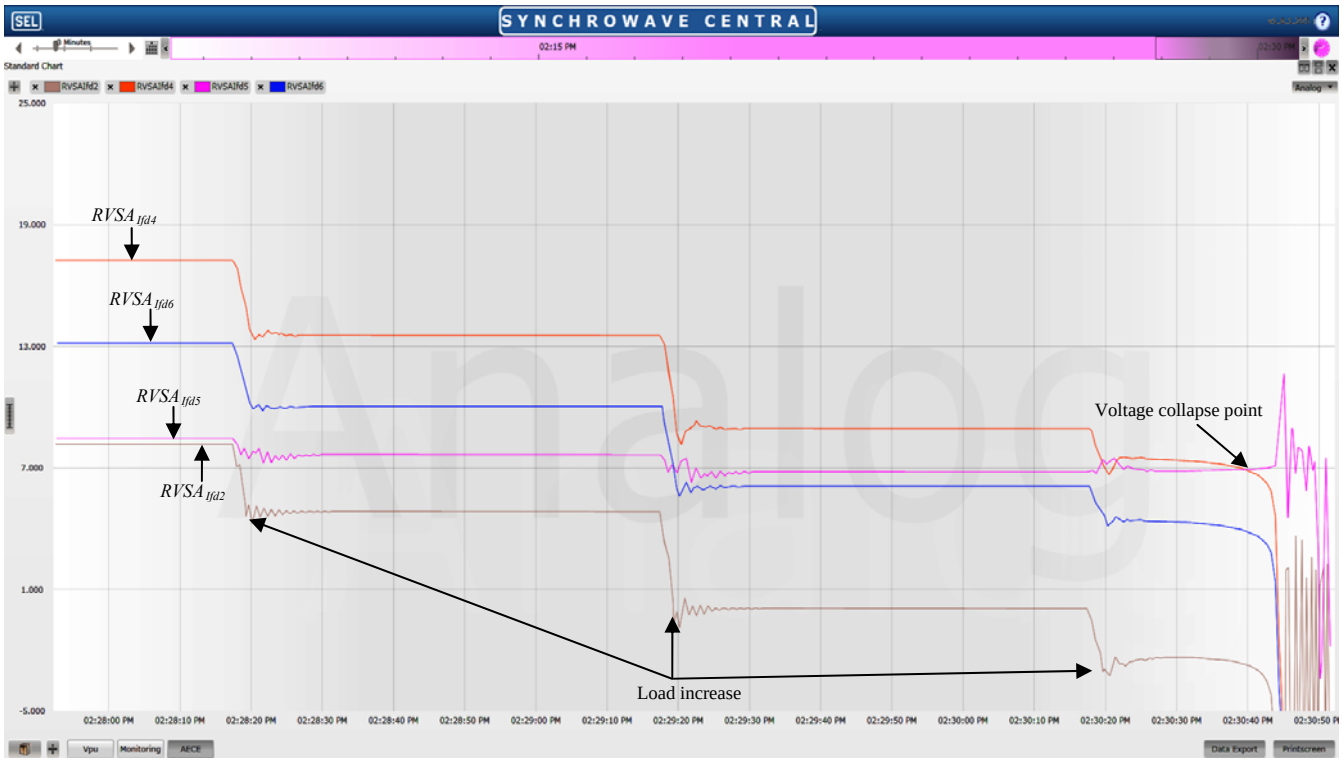

Figure 15. Real-time plot of $RVSA_{tfd}$ index for the key generators in each cluster

APPENDIX B

The ULTC parameters for the transformer between buses 11 and 12 are given in Table B1.

TABLE B1. TRANSFORMER ULTC PARAMETERS

Dead band (V p.u.)	Tap range (steps)	Step size (p.u.)	Time delay for 1st tap (s)	Time delay for other taps (s)
±1%	±16	0.00625	30	5

REFERENCES

[1] P. Kundur. Power System stability and control. McGraw-Hill, 1994.

[2] R. A. Schlueter, "A voltage stability security assessment method," IEEE Transactions on Power System, vol. 13, pp. 1423–1438, Nov. 1998. [Online]. Available: http://dx.doi.org/10.1109/59.736286

[3] A. Mohamed, G. B. Jasmon, S. Yusoff, "A static voltage collapse indicator using line stability factors," Journal of Industrial Technology, vol. 7, no. 1, pp. 73-85, 1989.

[4] M. Moghavvemi, O. Faruque, "Real time contingency evaluation and ranking technique," IEE Proceedings on Generation, Transmission and Distribution, vol. 145, no. 5, pp. 517–524, 1998. [Online]. Available: http://dx.doi.org/10..1049/ip-gtd:19982179

[5] I. Musirin, T. K. A. Rahman, "Implementation of FVSI for contingency ranking in power system," in proceedings, Australasian University Power Engineering Conference, Melborne, Australia, pp. 10-31, Sept. 29- Oct. 2 2002. [Online]. Available: http://dx.doi.org/10.1109/TDC.2002.1177634

[6] F. Capitanescu, T. Van Cutsem, "Evaluation of reactive power reserves with respect to contingencies," in proceedings, Bulk Power System Dynamic and Control V, 2001.

[7] Y. H. Choi, S. Seo, S. Kang, B. Lee, "Justification of effective reactive power reserves with respect to a particular bus using linear sensitivity," IEEE Transactions on Power Systems, vol. 26, no. 4, pp. 2118-2124, November 2011. [Online]. Available: http://dx.doi.org/10.1109/TPWRS.2011.2151212

[8] B. Leonardi, V Ajjarapu, "An approach for real time voltage stability margin control via reactive power reserve sensitivities," IEEE Transactions on Power Systems, vol. 28, no. 2, pp. 615-625, May 2013. [Online]. Available: http://dx.doi.org/10.1109/TPWRS.2012.2212253

[9] O. Mousavi, M. Bozorg, R. Cherkaoui, "Preventive reactive power management for improving voltage stability margin," Electric Power Systems Research, vol. 96, pp. 36-46, 2013.

[10] A. C. Adewole, R. Tzoneva, "Real-time deployment of a novel synchrophasor-based voltage stability assessment algorithm," International Review of Electrical Engineering, vol, 9, no. 5, pp. 1021-1033, 2014. [Online]. Available: http://dx.doi.org/10.15866/iree.v9i5.3051

[11] J. H. Liu, C. C. Chu, "Long-term voltage instability detections of multiple fixed-speed induction generators in distribution networks using synchrophasors," IEEE Transactions on Smart Grid, vol. PP. issue 99, pp. 1-11, 2015. [Online]. Available: http://dx.doi.org/10.1109/TSG.2014.2379716, to be published.

[12] R. Podmore, "Identification of coherent generators for dynamic equivalents," IEEE Trans. Power Apparatus System, vol. 97, no. 4, pp. 1344–1354, July 1978. [Online]. Available: http://dx.doi.org/10.1109/TPAS.1978.354620

[13] J. Zaborszky, K. W. Whang, G. M. Huang, , L. J. Chiang, S. H. Lin, "A clustered dynamic model for a class of linear autonomous systems using simple enumerative sorting," IEEE Transactions On Circuits and Systems, vol. CAS-29, no. 11, pp. 747-758, Nov. 1982. [Online]. Available: http://dx.doi.org/10.1109/TCS.1982.1085095

[14] J. H. Chow, R. Galarza, P. Accari, W. W. Price. "Inertial and slow coherency aggregation algorithms for power system dynamic model reduction," IEEE Transactions on Power System, vol. 10, no. 2, pp. 680–685, May 1995. [Online]. Available: http://dx.doi.org/10.1109/59.387903

[15] H. Kim, G. Jang, K. Song, "Dynamic reduction of the large-scale power systems using relation factor," IEEE Transactions on Power Systems, vol. 19, pp. 1696–1699, August 2004. [Online]. Available: http://dx.doi.org/10.1109/TPWRS.2004.831697

[16] Y. Xue, M. Pavella, "Critical cluster identification in transient stability studies," in Proceedings, Inst. Elect. Eng. C, vol. 140, no. 6, pp. 481-489, Nov. 1993.

[17] C. Juarez, A. R. Messina, R. Castellanos, G. Espinosa-Pérez "Characterization of multimachine system behavior using a hierarchical trajectory cluster analysis," IEEE Transactions On Power Systems, vol. 26, no. 3, pp. 972-981, August 2011. [Online]. Available: http://dx.doi.org/10.1109/TPWRS.2010.2100051

[18] R. Nath, S. S. Lamba, K. S. Prakasa Rao, "Coherency based system decomposition into study and external areas using weak coupling," IEEE Transactions on Power Apparatus and Systems, PAS-104, no. 6, pp. 1443-1449, 1985. [Online]. Available: http://dx.doi.org/10.1109/TPAS.1985.319158

[19] R. Agrawal, D. Thukaram, "Support vector clustering-based direct coherency identification of generators in a multi-machine power system," IET Generation Transmission Distribution, vol. 7, no. 12, pp. 1357–1366, 2013. [Online]. Available: http://dx.doi.org/10.1049/iet-gtd.2012.0681

[20] M. A. M. Ariff, B. C. Pal, "Coherency identification in interconnected power system-an independent component analysis approach." IEEE Transactions On Power Systems, vol. 28, no. 2, pp. 1747-1755, May 2013. [Online]. Available: http://dx.doi.org/10.1109/PESMG.2013.6672186

[21] J. Wei, D. Kundur, K. L. Butler-Purry, "A novel bio-inspired technique for rapid real-time generator coherency identification," IEEE Transactions on Smart Grid, pp. 1-11, 2014. [Online]. Available: http://dx.doi.org/10.1109/TSG.2014.2341213

[22] M. Jonsson, M. Begovic, J. Daalder, "A new method suitable for real-time generator coherency determination," IEEE Transactions on Power Systems, vol. 19, no. 3, pp. 1473–1482, Aug. 2004. [Online]. Available: http://dx.doi.org/10.1109/TPWRS.2004.826799

[23] I. Kamwa, A. K. Pradhan, G. Joo, S. R. Samantaray, "Fuzzy partitioning of a real power system for dynamic vulnerability assessment," IEEE Transactions on Power Systems, vol. 24, no. 3, pp. 1356-1365, August 2009. [Online]. Available: http://dx.doi.org/10.1109/TPWRS.2009.2021225

[24] K. Mei, S. M. Rovnyak, and C. M. Ong, "Clustering-based dynamic event location using wide-area phasor measurements," IEEE Transactions On Power Systems, vol. 23, no. 2, pp. 673-679, May 2008. [Online]. Available: http://dx.doi.org/10.1109/TPWRS.2008.920199

[25] A. C. Zambroni de Souza, V. H. Quintana, "New technique of network partitioning for voltage collapse margin calculations," IEE Proc-Gener. Transm. Distrib., vol. 141, no. 6, pp. 630-636, November 1994. [Online]. Available: http://dx.doi.org/10.1049/ip-gtd:19941491

[26] A. Nuhanovic, M. Glavic N. Prljaca, "Validation of a clustering algorithm for voltage stability analysis on the Bosnian electric power system," IEE Proc Gener. Transm. Distrib., vol. 145, no. 1, pp. 21-26, January 1998. [Online]. Available: http://dx.doi.org/10.1049/ip-gtd:19981266

[27] C. A. Aumuller, T. K. Saha, "Determination of power system coherent bus groups by novel sensitivity-based method for voltage stability assessment," IEEE Transactions on Power Systems, vol. 18, no.3, pp. 1157–1164, Aug. 2003. [Online]. Available: http://dx.doi.org/10.1109/TPWRS.2003.814886

[28] F. Rameshkhah, M. Abedi, S. H. Hosseinian, "Clustering of voltage control areas in power system using shuffled frog-leaping algorithm," Electrical Engineering, vol. 92, pp.269–282, 2010. [Online]. Available: http://dx.doi.org/10.1007/s00202-010-0178-y

[29] C37.118.1-2011, IEEE standard for synchrophasor measurements for power systems. [Online]. Available: http://dx.doi.org/10.1109/IEEESTD.2011.6111219

[30] C37.118.2005, IEEE standard for synchrophasor measurements for power systems. [Online]. Available: http://dx.doi.org/10.1109/IEEESTD.2006.99376

[31] C37.118.1a-2014, IEEE standard for synchrophasor measurements for power systems-amendment 1: modification of selected performance requirements. [Online]. Available: http://dx.doi.org/10.1109/IEEESTD.2014.6804630

[32] W. Hardle, L. Simar. Applied multivariate statistical analysis.2 ed. Springer-Verlag, 2007.

[33] R. A. Johnson, D. W. Wichern. Applied multivariate statistical analysis. 6 ed. Pearson Prentice-Hall, USA: NJ, 2007.

[34] MATLAB Statistic Toolbox: User's Guide, The MathWorks, Inc., Natick, Massachusetts, 2014.

[35] T. Calinski, J. Harabasz. "A dendrite method for cluster analysis," Communications in Statistics, vol. 3, no. 1, pp. 1–27, 1974. [Online]. Available: http://dx.doi.org/10.1080/03610927408827101

[36] F. Capitanescu, T. Van Cutsem, "Evaluation of reactive power reserves with respect to contingencies," in proceedings, Bulk Power System Dynamic and Control V, 2001.

[37] L. Bao, Z. Huang, W. Xu, "Online voltage stability monitoring using VAr reserves," IEEE Transactions on Power Systems, vol. 18, no. 4, pp. 1461-1469, Nov. 2003. [Online]. Available: http://dx.doi.org/10.1109/TPWRS.2003.818706

[38] F. Dong, B. H. Chowdhury, M. L. Crow, L. Acar. "Improving voltage stability by reactive power reserve management," IEEE Transactions on Power Systems, vol. 20, no. 1, pp. 338-344, 2005. [Online]. Available: http://dx.doi.org/10.1109/TPWRS.2004.841241

[39] Y. H. Choi, S. Seo, S. Kang, B. Lee, "justification of effective reactive power reserves with respect to a particular bus using linear sensitivity," IEEE Transactions on Power Systems, vol. 26, no. 4, pg. 2118-2124, November 2011. [Online]. Available: http://dx.doi.org/10.1109/TPWRS.2011.2151212

[40] C. W. Taylor, R. Ramanathan, "BPA reactive power monitoring and control following the August 10, 1996 power failure," in Proceedings, VI Symp. Specialists Elect. Operation Expansion Planning, Salvador, Brazil, May 24–29, 1998.

[41] B. Leonardi, V. Ajjarapu, "Investigation of various generator reactive power reserve (GRPR) definitions for online voltage stability/security assessment," in proceedings,Power and Energy Soc. Gen. Meet. – Convers. and Deliv. of Electr. Energy in the 21st Century, pp. 1–7. 2008. [Online]. Available: http://dx.doi.org/10.1109/PES.2008.4596235

[42] M. A. Pai. Energy function analysis for power system stability. Boston: Kluwer Academic Publishers, pp. 223-227, 1989.